RAPID COMMUNICATIONS

PHYSICAL REVIEW C VOLUME 49, NUMBER 5 MAY 1994

Excitation function for $^4He(\pi^+, pp)^2H$ two-nucleon absorption across the Δ resonance

H. Breuer, M. G. Khayat, F. Adimi, B. S. Flanders,*
M. A. Khandaker,† P. G. Roos, and D. Zhang‡
Department of Physics, University of Maryland, College Park, Maryland 20742

Th. S. Bauer§ and J. Konijn
NIKHEF-K, P.O. Box 4395, NL 1009 AJ Amsterdam, The Netherlands

C. T. A. M. de Laat
Physics Laboratory, University Utrecht, P.O. Box 80000, 3508 TA Utrecht, The Netherlands

G. S. Kyle, S. Mukhopadhyay,‖ and M. Wang¶
Department of Physics, New Mexico State University, Las Cruces, New Mexico 88003

R. Tacik**
University of Karlsruhe, 7500 Karlsruhe, Germany
(Received 23 December 1993)

Angular distributions and total cross sections for the $^4He(\pi^+, pp)^2H$ reaction have been measured with small relative uncertainties at incident energies of T_{π^+}=64, 87, 114, 162, 217, 278, and 327 MeV. The results strongly support the quasideuteron absorption model for pion absorption on two nucleons, which is found to contribute only $\approx$ 50% to the total absorption cross section near the Δ resonance. All essential reaction channels of pion absorption near the Δ resonance on heavier nuclei seem to be present in ^4He, but not in ^3He. Any nuclear-density-related increase of pion absorption in ^4He relative to ^2H is <50% and no binding energy effect is found.

PACS number(s): 25.80.Ls, 27.10.+h, 21.45.+v, 24.10.−i

The only single reaction channel that has been found to represent a major fraction of the pion absorption cross section near the Δ resonance is the two nucleon absorption (2NA) process, in which the pion is absorbed on a proton-neutron (pn) pair with the remainder of the target acting as a spectator. A large number of experiments have identified this process in a variety of $A \geq 3$ nuclei, e.g., ^3H, ^3He [1–4], ^4He [4–8], ^6Li [9–11], ^{16}O [12–15], and ^{58}Ni [16]. However, with the exception of π^+ absorption on the lightest two systems ^2H [17] and ^3He, no detailed 2NA cross section data as a function of the pion energy have been published to date.

The similarity of the angular distributions and energy dependence of the 2NA cross section data from ^2H and ^3He targets suggests that the absorption mechanism is essentially the same for these targets. The 2NA yield is about 50% larger for ^3He than for ^2H, in accordance with a simple counting of the number of $^3S_1$, $T = 0$ pn pairs available in the $A = 3$ system. In contrast, the ratio of the 2NA cross section for ^{16}O to that for ^2H at three pion energies [12–14] decreases with pion energy. At the peak of the Δ resonance 2NA contributes about 80% to the total absorption cross section in ^3He, while for ^{16}O this fraction is only about 50%. These observations suggest significant changes in the absorption mechanisms between $A = 3$ and $A = 16$ targets.

Compared to ^3He, even ^4He has many more reaction channels open for pion absorption [4,5]. In addition, any density or binding energy dependency of the 2NA process may become visible in the "real nucleus" ^4He. Thus, this $A = 4$ nucleus provides an important testing ground for the transition from pion absorption in a few-nucleon system to that in a multi-nucleon system. In this paper we report the experimental results for the 2NA cross section in ^4He at seven π^+ energies (64, 87, 114, 162, 217, 278, and 327 MeV), covering in a single experiment and with common systematic uncertainties nearly the full extent of the Δ-resonance energy region.

The experiment was performed using the πM1 channel positive pion beam of the Paul Scherrer Institut. The liquid ^4He target was contained in a large solid angle cryogenic target cell [18] surrounded by 16 plastic ΔE-E scintillator telescopes (ΔE: 102 × 20 × 1 cm^3, E: 100 × 18 × 18 cm^3) arranged approximately as a vertical cylinder. At ΔE detector distances between 477 and 710 mm the setup covered scattering angles between 7° and

*Present address: Dept. of Physics, American University, Washington, D.C. 20016.
†Present address: Physics Dept., Brookhaven National Laboratory, Upton, NY 11973.
‡Present address: Petrophysical Engineering, Shell Development, P.O. Box 482, Houston, TX 77001.
§Present address: Physics Laboratory, University Utrecht, P.O. Box 80000, 3508 TA Utrecht, The Netherlands.
‖Present address: Dept. of Physics, California State University, 5151 State University Drive, Los Angeles, CA 90032.
¶Present address: Dept. of Medical Physics, 1530 Medical Science Center, 1300 University Avenue, Madison, WI 53706.
**Present address: Dept. of Physics, University of Regina, Regina, SK, S4S OA2, Canada.

157° in the laboratory system and subtended 55% of 4π (with only 48% of 4π used here to minimize edge effects).

Detailed information about the experiment and analysis can be found in Adimi *et al.* [6]. Deviating from Ref. [6], the present analysis uses a conversion from energy loss to total particle energy for those protons which are not fully stopped in the detectors. The yield for such protons becomes important at T_π=162 MeV (reanalyzed here for consistency) and higher pion energies. The resolution for the summed energy, $E_{\rm sum} = E_{p1} + E_{p2} + E_{^2{\rm H}}$, given in Table I, reflects the uncertainties of this energy recovery procedure. To select only those events which are dominated by pure 2NA, only data satisfying gates on missing momentum, $k_{\rm miss} = \mid \mathbf{k}_\pi - \mathbf{k}_{p1} - \mathbf{k}_{p2} \mid <$ 250 MeV/c, and on missing energy, $E_{\rm miss} = E_{^4{\rm He}} + E_\pi - E_{\rm sum}$, have been used. Here E and k represent the total energy and momentum, respectively, of ^{4}He, ^{2}H, and the two detected protons, $p1$ and $p2$. The threshold on the proton kinetic energy was set in software to be 18 MeV at the center of the target.

The data have been modeled in a Monte Carlo (MC) simulation (computer code GEANT [19]) which includes all features of the experimental geometry and resolution and the Fermi motion of the absorbing nucleon pair in the target nucleus [6]. The code also incorporates the ^{2}H(π^+,pp) differential cross sections in a plane wave impulse approximation treatment of the absorption process [6,20] using a parametrization [17] of the energy and angle dependence of the ^{2}H(π^+,pp) cross section. The excellent agreement between experiment and simulation can be observed in [6].

The cross sections, including all extrapolations into unmeasured regions of phase space, are obtained by normalizing the experimental data with the MC generated data after both have been analyzed with identical procedures [6]. Note that any arbitrary choice of gates necessarily yields identical cross sections as long as the MC model is a perfect representation of the experimental data [6]. It is found that the extracted cross sections are actually rather insensitive to variations in the MC simulation, which is a consequence of the large solid angle coverage.

Figure 1 shows a selection of the angular distributions for the ^{4}He experimental cross section data as well as the corresponding MC generated data. In general, very good agreement between experiment and MC is visible. A detailed inspection of Fig. 1, however, reveals some important differences between the experimental and the MC data. These differences are quantified in Fig. 2, where the ratio of the coefficients a_2 and a_0 from Legendre polynomial fits to the data $[\sum_i a_i P_i(\cos\Theta);\ i = 0,2,4,6]$ have been plotted. The ratios for the MC data decrease smoothly with energy, only slightly changed from those of the ^{2}H(π^+,pp) input data by the effects of Fermi motion and experimental resolution. In contrast, although scattered rather strongly, the experimental a_2/a_0 ratios are clearly larger than the MC predictions at high energies. Fits up to order $i = 8$ give equivalent results. Similar to our ^{4}He data, a nearly constant a_2/a_0 ratio is apparent for ^{3}He(π^+,pp) up to T_{π^+}=206 MeV (Table 15 of Ref. [4]).

It is unlikely for this energy region that the discrepancy between experimental and MC data reflects an imperfect parametrization of the ^{2}H 2NA angular distributions [17]

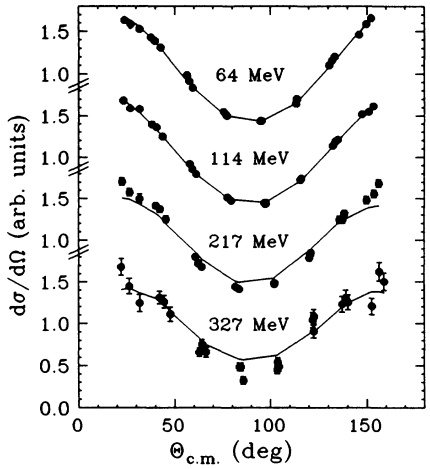

FIG. 1. Angular distributions of 2NA cross sections from ^{4}He(π^+,pp) at four pion kinetic energies in the center of mass of the π-^{2}H system. Circles represent experimental data. Position gates on the detectors have been used to obtain more data points than the number of detectors. Curves are from MC simulations, see text.

TABLE I. Results from the 2NA reaction ^{4}He(π^+,pp)^{2}H between T_π=64 and 327 MeV. $\sigma_{^4{\rm He}}$ are 2NA cross sections, extracted using $k_{\rm miss}$ and $E_{\rm miss}$ conditions as discussed in the text. Values with an asterisk are based on $E_{\rm miss}$<30 MeV, see text. The uncertainties shown contain the statistical errors and calibration uncertainties specific to the particular energy. In addition, and not included, is the 6.5% systematic normalization uncertainty which is identical for all energies. RES($E_{\rm sum}$) represents the variance of the 2NA absorption peak in the summed energy spectrum. $\sigma^{\rm FSI}_{^4{\rm He}}$ are 2NA cross sections corrected for FSI effects (±15% uncertainty for the FSI correction factor). Values for $\sigma_{^2{\rm H}}$ are from Ref. [17]. The last row gives $\sigma^{\rm abs}_{^4{\rm He}}$ values used in Fig. 4(b).

	Pion kinetic energy (MeV)						
	64	87	114	162	217	278	327
$\sigma_{^4{\rm He}}$ (mb); $E_{\rm miss}$<30 MeV	17.7	22.7	26.7	21.5	11.9	6.1	3.8
$\sigma_{^4{\rm He}}$ (mb); $E_{\rm miss}$<12 MeV	16.9	22.0	25.8	20.5	11.5	5.9*	3.7*
Uncertainty (%)	±3.1	±6.5	±2.9	±4.1	±5.2	±5.9	±8.8
RES($E_{\rm sum}$) (MeV)	±7.5	±8.2	±9.0	±10.5	±14.4	±20.7	±31.8
$\sigma^{\rm FSI}_{^4{\rm He}}$ (mb); $E_{\rm miss}$<12 MeV	23.3	31.2	37.5	30.7	17.9	9.4*	6.0*
$\sigma^{\rm FSI}_{^4{\rm He}}/\sigma_{^2H}$; $E_{\rm miss}$<12 MeV	3.35	3.37	3.21	2.90	3.35	3.58*	3.83*
$\sigma^{\rm abs}_{^4{\rm He}}$ (mb)	32/45	49/71	64/84	59/76	41/41	33/33	31/31

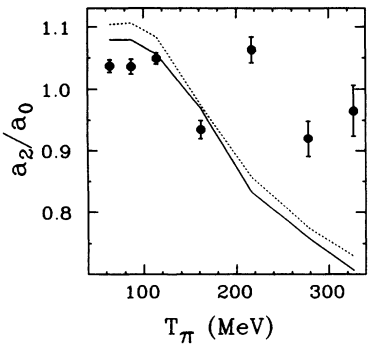

FIG. 2. Ratios of the coefficients a_2/a_0 of a sixth-order Legendre polynomial fit to the data in Fig. 1. Circles are from the experimental data, the solid line is from MC simulations. The dotted line represents a_2/a_0 for ^{2}H(π^+,pp) from Ref. [17].

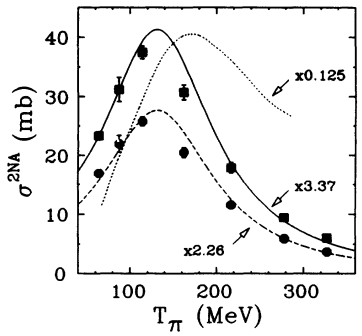

FIG. 3. Excitation function for 2NA of pions in ^{4}He. Directly measured data (circles) and measured data corrected for FSI losses (squares) are compared with dashed and solid curves which represent ^{2}H(π^+,pp) scaled by the factors indicated [17]. The dotted line represents the scaled total cross sections for all pion interactions [27,28].

included in the MC simulations. The deviations could be a reflection of distortion effects for the outgoing protons due to the residual nucleus. In addition, the angular distribution could be modified by the presence of non-$^3S_1$ *pn*-pair absorption processes; e.g., absorption on a $T = 1$ *pn* pair is expected to be relatively more important at off-resonance energies. The details of the angular distributions may be a sensitive indicator for such processes. At T_π=870 MeV [21] a_2/a_0 for ^{4}He(π^+,pp) appears to be much larger than for ^{2}H(π^+,pp), consistent with the trend of the current data. In contrast, at T_π=500 MeV the ^{2}H(π^+,pp) angular distribution, scaled by 3.0, gives an excellent fit to the ^{4}He(π^+,pp) angular distribution [7].

The cross sections extracted for 2NA of pions in ^{4}He are given in Table I for data with $E_{\rm miss}$ of less than 12 and 30 MeV, respectively. For $E_{\rm miss}$<12 MeV the data are practically free of events from non-2NA absorption processes [6]. To minimize the calibration uncertainties originating from the worsened energy resolution at 278 and 327 MeV, cross sections for these data have been extracted for $E_{\rm miss}$<30 MeV only. An estimate of the pure 2NA cross section ($E_{\rm miss}$<12 MeV) is obtained by reducing the 30 MeV gate result by 4%, the average difference between the results with the two $E_{\rm miss}$ gates at the lower beam energies.

Factors needed to correct the measured data for final state interaction (FSI) effects have been obtained from distorted wave impulse approximation calculations done with and without the imaginary part of the outgoing proton optical potential present [6,13,20]. The difference in these calculations represents the yield removed from the elastic channel for the outgoing protons by the imaginary potential or, equivalently, by all nonelastic FSIs. These factors, increasing with pion energy from 1.38 to 1.63 over the range of the data and with estimated uncertainties of ±0.2 [7,13,14,22], have been applied to the 12 MeV gate data to obtain the FSI corrected cross sections given in Table I.

Figure 3 presents the 2NA cross sections, σ^{2NA}, on ^{4}He as a function of incident pion energy with (squares) and without (circles) FSI corrections. Also shown as curves are the ^{2}H(π^+,pp) cross sections [17] scaled by the factors indicated. The 2NA excitation functions for ^{4}He and ^{2}H are nearly identical in shape. This applies both to the directly measured and the FSI corrected data since the FSI factors vary slowly with pion energy. It should be emphasized that the shape of the excitation functions of ^{4}He and ^{2}H are so similar in spite of the fact that *pn* pairs are bound in ^{4}He by 23 MeV. The peak would occur about 20 MeV higher for ^{4}He than for ^{2}H if the *pn* pair was removed from the ^{4}He before the absorption (the "final energy prescription" in an impulse approximation treatment of the reaction [14,20]). Instead, the data suggest that the peak is slightly lower in energy, more in agreement with the "initial energy prescription" [14].

Taking the ^{2}H curve in Fig. 3 as a reference, the data point at 162 MeV and, to a lesser degree, at 114 MeV have reduced cross sections. Pion-induced reactions, including 2NA, are dominated at these energies by the entrance channel doorway state of Δ formation. This is, for example, evident from the shape of the total reaction cross section [27,28] (dotted line in Fig. 3). The suppressed σ^{2NA} could be due to a modification of the partial decay width of the Δ into 2NA near the peak of the resonance. This explanation is, however, not supported by the energy dependence of the cross section ratio of 2NA to total absorption discussed below. It is more likely that at the energies with the highest cross sections even a small nucleus like ^{4}He is no longer fully transparent so that shadowing prevents some nucleons from participating fully in the formation of the initial Δ and thus also reduces the 2NA yield. The dotted line in Fig. 3 shows that the total cross section peaks near the 162 MeV point, consistent with a maximum amount of shadowing at this energy. It is interesting to note that this behavior of reduced 2NA strength at energies of 115 MeV and beyond seems to be much more pronounced in ^{16}O [14].

The ratio of σ^{2NA} for ^{4}He (FSI corrected) to ^{2}H ranges from 2.9 to 3.8 (Table I). This is, on the average, somewhat larger than the 3.0 quasideuteron pairs expected for a naive model of ^{4}He and consistently higher than the ratio of 2.4 estimated from structure calculations by Schiavilla *et al.* [23]. Two effects have to be taken into account for a quantitative interpretation of these

ratios: (a) the 2NA cross sections have to be reduced by the absorption on $^1S_0$ ($T = 1$) pn pairs (and possibly by higher l components) to obtain the $^3S_1$ ($T = 0$) component, and (b) the cross sections have to be corrected (increased) for any nuclear shadowing effects. A ratio of $\sigma^{2NA}(T = 1)/\sigma^{2NA}(T = 0) \approx 0.05$ has been measured by Steinacher *et al.* [5] at 120 MeV. Assuming an energy-independent $\sigma^{2NA}(T = 1)$ background of $0.05\sigma^{2NA}(114\ \text{MeV}) = 1.9$ mb yields an average ratio of 3.1 for the lowest three energies and smaller values at the higher energies. Neglecting any possible shadowing effects (which should be minimized at the lowest energies, Fig. 3) and using the 2.4 quasideuterons in ^{4}He of Ref. [23] as a basis, one finds that the $^3S_1$ absorption cross section is enhanced by 30% relative to the elementary ^{2}H(π^+,pp) reaction. Taking all uncertainties into account, the present data would be consistent with a 0 to 50% increase in the $^3S_1$ pn-pair absorption strength in ^{4}He relative to ^{2}H.

The ratio of 2NA to the total absorption cross section, $\sigma^{2NA}/\sigma^{abs}$, can reveal the significance of non-2NA channels, which are possible in $A \geq 3$ nuclei. Figure 4(b) shows the present 2NA data divided by the total absorption cross section, $\sigma^{abs}_{^4He}$ [24]. The error bars are dominated by the rather large $\sigma^{abs}_{^4He}$ uncertainties, making detailed and definite statements about the energy dependence difficult. The results in Fig. 4(b) are consistent with a continuous decrease with energy of the 2NA fraction from about 70% to 20% over the energy range covered here. However, the uncertainty in $\sigma^{abs}_{^4He}$ also allows for the possibility of a constant 40% to 50% 2NA component up to $T_\pi \approx 220$ MeV. What is evident is that non-2NA processes play a very significant role at all energies in π^+ absorption on ^{4}He and may dominate absorption at energies well above the Δ resonance.

Figure 4 also shows $\sigma^{2NA}/\sigma^{abs}$ ratios for ^{6}Li and ^{16}O. All three $A \geq 4$ targets have values of about 50% near the peak of the Δ resonance (when corrected for FSIs) and the energy dependence may be about the same. The calculations by Oset [25], performed for ^{12}C (lines in Fig. 4), are consistent with all data for $A \geq 4$ shown in Fig. 4. In contrast, for ^{3}He below E_{π^+}=250 MeV, $\sigma^{2NA}/\sigma^{abs}$ is about 80% and nearly independent of energy [Fig. 4(a)]. Thus, for ^{3}He, three-nucleon absorption processes increase σ^{abs} by about 30% over σ^{2NA}. Our ^{4}He data, combined with published σ^{abs} values, indicate that the additional reaction channels available when adding a fourth nucleon even increase σ^{abs} by about 100% relative to σ^{2NA}. However, adding further nucleons and even more possible reaction channels does not change the non-2NA contribution further.

In summary, this experiment provides angular distributions and the excitation function of the cross section for 2NA over a wide range of pion energies in the ^{4}He(π^+,pp) reaction with small relative uncertainties. Due to the large solid angle coverage of the detectors, the results have little sensitivity to model assumptions and to extrapolations of the data. The angular distributions and the excitation function of the 2NA cross section are described very well by model MC simulations which include the energy and angle dependence of the ^{2}H(π^+,pp) process, indicating the importance and supporting the validity of the quasideuteron absorption (QDA) model. Considering the four times higher density (based on the rms charge radius [23]) and correspondingly smaller average separation of protons and neutrons in ^{4}He as compared to ^{2}H, one might expect a strong modification of the 2NA process in ^{4}He. If any such density dependence exists, it enhances the 2NA cross section by less than about 50%. No evidence is found that the 23 MeV separation energy for a pn pair in ^{4}He has any impact on the 2NA process. Small deviations from the QDA model predictions are seen in the cross section near the peak of the Δ resonance, possibly due to nuclear shadowing. Differences between experiment and MC observed in the angular distributions may originate from non-$^3S_1$ pn-pair absorption processes. The data imply that more complex absorption processes than 2NA must play an important role practically at all energies investigated. This feature sets ^{4}He apart from the $A = 3$ systems where 2NA strongly dominates, and puts it into the same class as complex nuclei like ^{6}Li and ^{16}O. For ^{4}He the amount of non-2NA indicated by the present experiment appears to be larger than expected from a previous experiment [5], which obtained cross sections at T_π=120 MeV for many reaction channels, but which required large extrapolations into unmeasured regions of phase space.

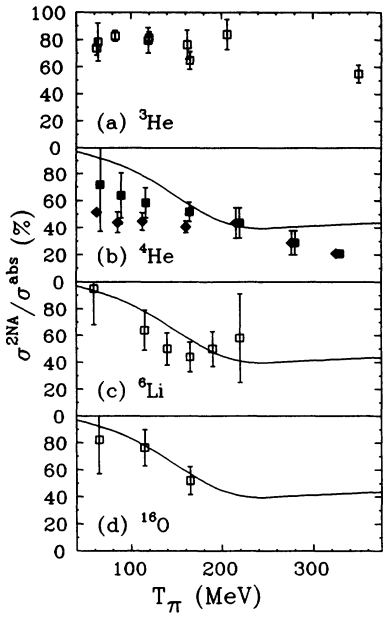

FIG. 4. Ratio of the FSI corrected 2NA cross section to the total absorption cross section, $\sigma^{2NA}/\sigma^{abs}$, as a function of pion kinetic energy, T_π. For ^{3}He, σ^{abs} is taken as $\sigma^{2NA}+\sigma^{3NA}$ from Ref. [2,3]. For ^{4}He, σ^{abs} is extracted from Fig. 19 of Ref. [24] from two smooth curves through the two data sets (values are given in Table I), resulting in the ratios given by squares and diamonds, respectively (offset for clarity by ± 2 MeV each). The errors on $\sigma^{abs}_{^4He}$ are taken from the closest σ^{abs} data points. Points without error bars use extrapolations from the data of Ref. [24]. $\sigma^{2NA}_{^6Li}/\sigma^{abs}_{^6Li}$ are from Refs. [9,10], and $\sigma^{2NA}_{^{16}O}/\sigma^{abs}_{^{16}O}$ are from Ref. [14]. All curves are the prediction for a ^{12}C target by Oset *et al.* [25].

It has been observed previously that $\sigma^{abs}(A)$ at T_π=165 MeV increases strongly with target mass between $A = 2$ and $A = 4$ or 6 followed by a more moderate increase $\sim A^{0.7}$ [2,26]. Based on our data, these observations are consistent with the following interpretation. For $2 \leq A \leq 4$ essentially all target nucleons participate in absorption with non-2NA increasing from 0% to about 50%. To a small degree for ^{4}He, and very strongly for heavier nuclei, shadowing effects limit σ^{abs} to be proportional to the geometric cross section, reducing both 2NA and non-2NA by similar amounts from values expected purely on the basis of nucleons or nucleon multiplets available. While the fraction of non-2NA increases strongly between $A = 3$ and $A = 4$, the data suggest that all significant absorption modes are already present in the $A = 4$ nucleus, based on a constant fraction of about 50% 2NA for $A = 4$, 6, and 16.

We thank the staff at PSI for the beam and the logistic support, B. van den Brandt and J. A. Konter for the help with the liquid-He supply system, and Y. Lefevere for the construction of the cryogenic target and his help with the detector setup. We thank J. Visschers for his contributions during the design stage and N. S. Chant for valuable discussions. The experiment was supported in part by the U.S. NSF and DOE.

[1] P. Salvisberg *et al.*, Phys. Rev. C **46**, 2172 (1992).
[2] S. Mukhopadhyay *et al.*, Phys. Rev. C **43**, 957 (1991), and references therein.
[3] P. Weber *et al.*, Nucl. Phys. **A501**, 765 (1989); P. Weber *et al.*, *ibid.* **A534**, 541 (1991).
[4] H. J. Weyer, Phys. Rep. **195**, 295 (1990).
[5] M. Steinacher *et al.*, Nucl. Phys. **A517**, 413 (1990).
[6] F. Adimi *et al.*, Phys. Rev. C **45**, 2589 (1992).
[7] L. C. Smith *et al.*, Phys. Rev. C **48**, R485 (1993).
[8] P. Weber *et al.*, Phys. Rev. C **43**, 1553 (1991).
[9] R. Rieder *et al.*, Phys. Rev. C **33**, 614 (1986).
[10] D. Zhang, Ph.D. thesis, University of Maryland, 1990.
[11] R. D. Ransome *et al.*, Phys. Rev. C **46**, 273 (1992); R. D. Ransome *et al.*, *ibid.* **45**, R509 (1992).
[12] Th. S. Bauer *et al.*, Phys. Rev. C **46**, R20 (1992).
[13] D. J. Mack *et al.*, Phys. Rev. C **45**, 1767 (1992).
[14] S. D. Hyman *et al.*, Phys. Rev. C **41**, R409 (1990); S. D. Hyman *et al.*, *ibid.* **47**, 1184 (1993).
[15] R. A. Schumacher *et al.*, Phys. Rev. C **38**, 2205 (1988).
[16] W. J. Burger *et al.*, Phys. Rev. Lett. **57**, 58 (1986); Phys. Rev. C **41**, 2215 (1990).
[17] B. G. Ritchie, Phys. Rev. C **44**, 533 (1991).
[18] Yke Lefevere, Jan H.M. Bijleveld, Martin Doets, Norbert Idskes, Thomas S. Bauer, Herbert Breuer, and Mahbubul A. Khandaker, Nucl. Instrum. Methods **A290**, 34 (1990).
[19] R. Brun, F. Bruyant, M. Maire, A. C. McPherson, and P. Zanarini, GEANT3, CERN program library, DD/EE/84-1 (1987).
[20] P. G. Roos, L. Rees, and N. S. Chant, Phys. Rev. C **24**, 2647 (1981); N. S. Chant and P. G. Roos, *ibid.* **39**, 957 (1989). The impulse approximation calculations were done using the computer code THREEDEE of N. S. Chant (unpublished).
[21] Izumi Nomura, RIKEN Internal Report RIKEN-AF-NP-110 (1991).
[22] G. Garino *et al.*, Phys. Rev. C **45**, 780 (1992).
[23] R. Schiavilla, V. R. Pandharipande, and R. B. Wiringa, Nucl. Phys. **A449**, 219 (1986).
[24] M. Baumgartner, H. P. Gubler, G. R. Plattner, W. D. Ramsay, H. W. Roser, I. Sick, P. Zupranski, J. P. Egger, and M. Thies, Nucl. Phys. **A399**, 451 (1983).
[25] E. Oset, Y. Futami, and H. Toki, Nucl. Phys. **A448**, 597 (1986).
[26] D. Ashery, I. Navon, G. Azuelos, H. K. Walter, H. J. Pfeiffer, and F. W. Schlepütz, Phys. Rev. C **23**, 2173 (1981).
[27] F. Binon, P. Duteil, M. Gouanére, L. Hugon, J. Jansen, J.-P. Lagnaux, H. Palevsky, J.-P. Peigneux, M. Spighel, and J.-P. Stroot, Nucl. Phys. **A298**, 499 (1978).
[28] C. Wilkin, C.R. Cox, J.J. Domingo, K. Gabathuler, E. Pedroni, J. Rohlin, P. Schwaller, and N.W. Tanner, Nucl. Phys. **B62**, 61 (1973).